Soft-x-ray emission of galliumlike rare-earth atoms produced by high-temperature low-density tokamak and high-density laser plasmas

K. B. Fournier, W. H. Goldstein, and A. Osterheld
Lawrence Livermore National Laboratories, P.O. Box 808, Livermore, California 94550

M. Finkenthal,* S. Lippmann,† L. K. Huang, and H. W. Moos
Department of Physics and Astronomy, The Johns Hopkins University, Baltimore, Maryland 21218

N. Spector
Soreq Nuclear Research Center, Yavneh 70600, Israel
(Received 24 March 1994)

Spectra of rare-earth atoms praseodymium, $Z=59$, to ytterbium, $Z=70$, emitted from the high-temperature (1 keV) low-density (10^{13} cm^{-3}) TEXT tokamak (at the Fusion Research Center, University of Texas, Austin) and high-density (10^{20} cm^{-3}) laser plasmas have been recorded in the soft-x-ray range of 50–200 Å with an image intensifier detector and on photographic plates. The brightest $n=4$ to $n=4$ transitions of galliumlike ions have been identified and their emission patterns have been studied by comparison with *ab initio* atomic structure calculations and collisional radiative models under the respective plasma conditions. We have investigated the use of the ratios of the intensities of 4-4 transitions as indicators of plasma densities. This is possible owing to the doublet structure of the galliumlike ground state, which leads to a strong density dependence for ratios of transitions between low-lying levels. We have also used semiempirical ionization balance calculations to characterize the charge state distribution of the tokamak plasmas, in preparation for an investigation of the use of ratios of galliumlike to zinclike and copperlike emission features as indicators of whether the impurities are in coronal equilibrium or undergoing ionization.

PACS number(s): 32.70.Fw, 32.30.Jc, 52.25.−b

INTRODUCTION

Soft-x-ray emission from rare-earth elements ($Z=58-71$) is of interest for its role in x ray laser and inertial confinement fusion experiments, and also for its potential as a bright x ray source for lithography and microscopy [1,2]. However, the main motivation for the present work is the potential use of galliumlike lines, together with adjacent copper- and zinclike lines, of the rare-earth ions as probes of transport phenomena in low-density, high-temperature tokamak plasmas. The relative intensity ratios of strong emission lines of copper-, zinc-, and galliumlike ions will differ depending on whether coronal equilibrium or transient ionizing (when particle transport is fast) conditions obtain, mainly owing to the effect of excitation-autoionization processes [3]. The temperatures of maximum abundance for the ions discussed here are affected by the inclusion of autoionization and dielectronic recombination processes in ionization equilibrium calculations. "Anomalous" values for the brightness ratios, i.e., ratios different from those obtained assuming that each ion emits at its temperature of max-

imum abundance, are indicative of rapid transport in the plasma.

Before exploring the use of rare-earth elements as probes of transport phenomena in low-density plasmas, we shall identify some $n=4$ to $n=4$ transitions between the lower energy levels in the galliumlike ions of the rare-earth atoms, and explain how to use the relative intensities of the spectroscopic emissions of heavy elements in high-temperature tokamak or laser-produced fusion plasmas to infer reliably the emitting plasma density. The ground-state doublet structure of the galliumlike charge state of the atoms in this study provides us with a mechanism to estimate local plasma densities. This work identifies the brightest lines of galliumlike ions from Pr^{28+} to Yb^{39+} and examines the use of $\Delta n=0$ transitions within the $n=4$ shell of those ions as possible density diagnostics in high-temperature plasmas over a large range of electron densities, $10^{13}-10^{21}$ cm^{-3}.

The emission pattern of rare-earth elements between 50 and 2000 Å was first studied in low-energy laser-produced plasmas at temperatures between 50 and 200 eV [4]. The quasiband emission patterns seen by Carrol and O'Sullivan have been reproduced in a variety of sources, such as high-energy laser [5,6], spark [7], and tokamak [8] produced plasmas. All these spectra showed a band of quasicontinuum, resulting from the superposition of a very large number of individual transitions emitted by many charge states having $4p^6 4d^k$ or $4p^k$ ground configurations. Mandelbaum *et al.* discuss in detail the

---

spectral composition of this band in Ref. [7]. Charge states with relatively simple ground states, such as copper-, zinc-, and galliumlike ($4s$, $4s^2$, and $4s^2 4p$, respectively), dominate the emission spectra in plasmas with electron temperatures in excess of 500 eV. These charge states emit at wavelengths which in general are longer than the wavelengths of the bands.

Resonance copper- and zinclike lines of praseodymium, europium, gadolinium, dysprosium, and ytterbium have been identified in tokamak plasmas [9] while praseodymium, samarium, europium, gadolinium, and ytterbium have been studied in laser-produced plasmas [10,11]. Further, the intercombination lines of zinclike ions with $Z > 50$ [12] and other weak zinclike lines of samarium, gadolinium, dysprosium, and ytterbium in laser-produced plasma spectra [13,14] have been reported. However, for galliumlike ions, line identifications have been made only for lower-Z elements, namely, from Br V to In XIX [15–17].

Studies of galliumlike spectra for $Z \leq 49$ have resulted in a semiempirical linear parametrization of the $4s^2 4p\ {}^2P_{1/2} - {}^2P_{3/2}$ energy gap for all atoms from gallium to uranium, based on replacing the nuclear charge Z with a screened nuclear charge $Z - S(Z)$ in the hydrogenic ex-

pression for the $4p$ fine-structure separation [18]. The expression includes a high-order Sommerfeld expansion of the Dirac energy as well as quantum electrodynamics corrections [19]. This linearity is observed experimentally to hold for nuclear charges Z between 31 and 49 and demonstrated in calculations for Z up to 58, at which point relativistic effects in the atomic core cause a departure from linearity. Multiconfiguration Dirac-Fock calculations [20] have modeled this departure from linearity. Our calculations for the low-lying energy-level structure of the galliumlike rare-earth atoms studied here predict the same departure from linearity (see Fig. 1).

EXPERIMENTS

The rare-earth elements praseodymium ($Z = 59$), europium ($Z = 63$), gadolinium ($Z = 64$), dysprosium ($Z = 66$), and ytterbium ($Z = 70$) were introduced into the TEXT tokamak (at the Fusion Research Center, University of Texas, Austin) by the laser blow-off technique [21]. The most important parameters in the experiment are summarized as follows: a toroidal magnetic field of 28 kG, a plasma current of 300 kA during the flat top, a plasma major radius of 100 cm, and minor radius of 27
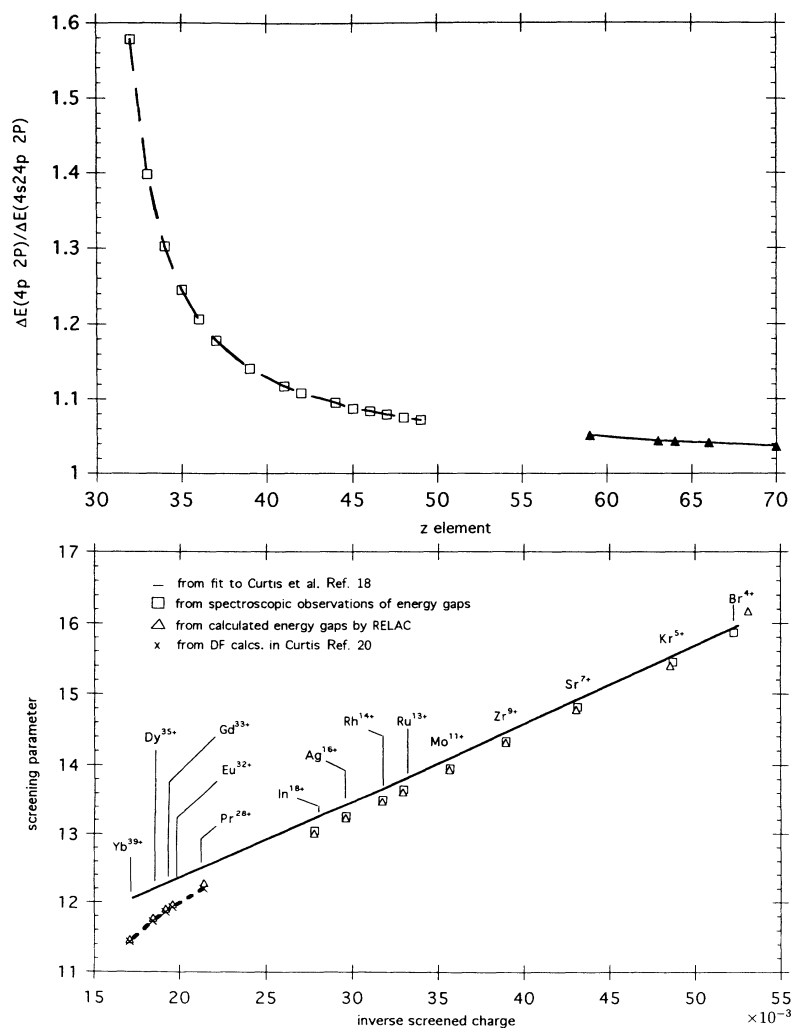

FIG. 1. (Top) The ratio of the fine-structure splitting in the $4p\ {}^2P$ term of copperlike ions to the $4s^2 4p\ {}^2P$ splitting in the ground term of galliumlike ions. The curve on the left comes from Fig. 2 in Ref. [15] and the points on the right come from RELAC calculations. (Bottom) Calculated screening parameter versus inverse screened charge. The observations (squares) and the semiempirical fit (line) found by Curtis et al. are in Ref. [18], the triangles are from RELAC calculations, and the Dirac-Fock values (×'s) are from Ref. [20]. Triangles and ×'s completely overlap.
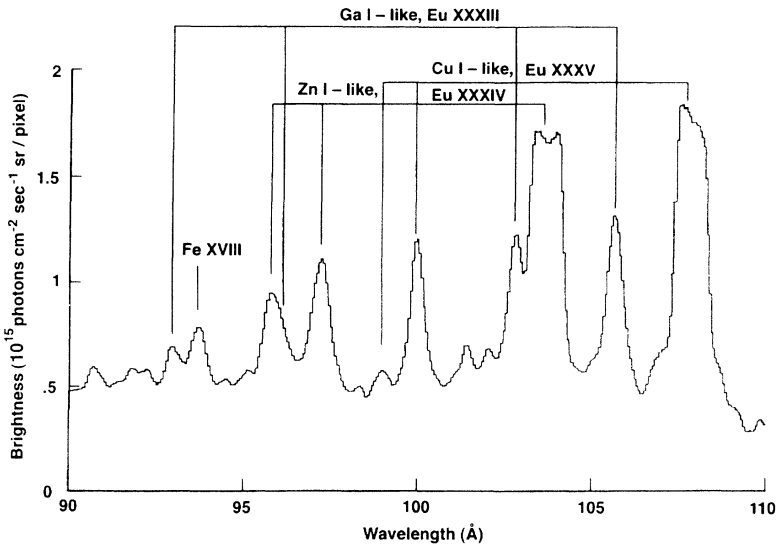
FIG. 2. Detailed europium spectrum emitted from TEXT tokamak plasma. The frame shown is that of peak galliumlike *e*-line emission. Transitions are labeled in Table I.

cm. The central electron temperature was 1 keV in most of the experiments (but up to 1.5–1.7 keV temperatures were reached in helium discharges) and the central electron density was 3.5×10^{13} cm^{-3}. The radial profiles of density and temperature are approximately Gaussian in shape; the electron temperature is maximum on axis and decreases to about 15 eV at the limiter radius [22].

The spectra were recorded by the grazing-incidence time-resolving spectrograph (GRITS) developed at the Johns Hopkins University [23]. The GRITS provides wavelength coverage from 50 to 360 Å and the detector may be moved along the Rowland circle to cover simultaneously a 40–80-Å region with a 0.7-Å resolution [line profile full width at half maximum (FWHM)]. The image intensifier detector on the experiment provided a 5.4-ms time integration of the incoming flux.

The instrument has been photometrically calibrated between 50 and 360 Å, using synchrotron radiation from the NIST SURF II electron storage ring. The uncertainty in the absolute brightness measurements due to scattered light, second-order contamination, and other effects is approximately 30%. A wavelength calibration was performed using a polynomial interpolation procedure between well-known lines of intrinsic (C, O, Ti, and Fe) and injected impurities in the tokamak discharge; estimated uncertainty in the determination of the wavelength of an unknown line is 0.2 Å. For most of the measurements reported here, the spectrograph viewed the plasma along a line of sight through its center.

Figure 2 is a detailed europium spectrum taken from the TEXT plasma in the wavelength range of 90 to 110 Å. The trace displayed is one taken during the frame of maximum copper- and zinclike emission from which the intrinsic background (the frame before the europium injection) has been subtracted.

In the laser experiments, a Nd-glass laser beam was focused on planar praseodymium, samarium, gadolinium, dysprosium, and ytterbium targets. The laser energy was 70 J and the pulse shape was a Gaussian of 3.5 ns (FWHM). The laser beam was focused to a spot size of several micrometers and the power density on the target

was of the order of 10^{14} W/cm^2. The pulse rate was about one shot every 20 min, and three to six shots were fired to obtain strong lines on the Kodak SC5 photographic plates. A 2-m grazing incidence Schwob-Fraenkel spectrograph [24] equipped with a 600-groove/mm grating allowed the recording of the spectrum over the 5–350 Å range. Its spectral resolution in this experiment was 0.01 Å. The recorded spectra in the
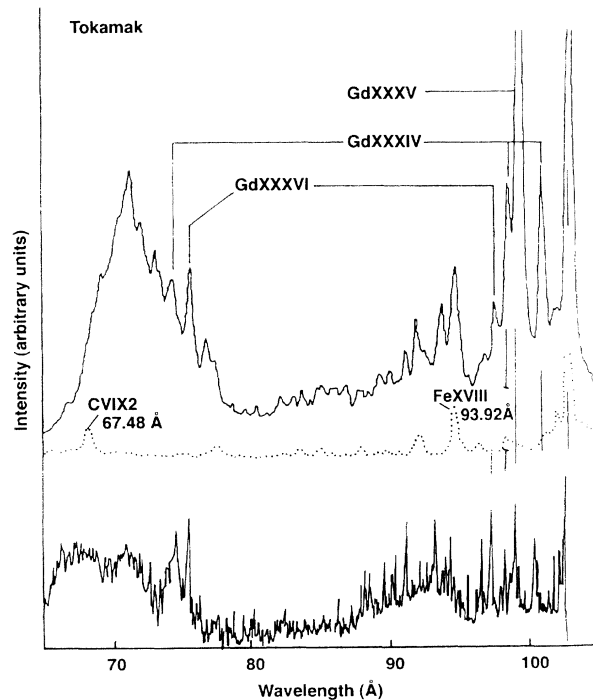

FIG. 3. Comparison of the soft-x-ray emission of gadolinium from a tokamak plasma (top) and a laser-produced plasma (bottom). The frame shown for the tokamak spectrum is that of maximum emission in the galliumlike *e* line. The dotted trace is that of the tokamak plasma's spectrum just prior to the injection of the gadolinium.

range of interest were analyzed by a microdensitometer and the relative intensities were determined from the measured photographic density. Although this spectrometer was not calibrated photometrically, the errors in the relative line intensities are less than 30% for lines separated by less than 5 Å in the spectrum.

Figure 3 shows two gadolinium emission spectra in the 70–100 Å range, one from the laser-produced plasma (bottom trace) and the second from the tokamak plasma (top trace). The gross character of the spectra reflects the very different densities of the emitting plasmas; the laser-produced plasma contains many more lines than the tokamak plasma, and their relative intensities are different than those of the tokamak spectrum. Finally, it should be noted that the time-resolved nature of the

TABLE I. Transitions from the excited configurations $4s4p^2$ and $4s^24d$ to the ground-state configuration $4s^24p$ in galliumlike ions. Numbers in parentheses are the total J value for the level; a subscript of $-$ or $+$ after an orbital quantum number indicates either $l-s$ or $l+s$ coupling in a jj-coupling scheme, respectively. For example, $4p_+$ would be a $4p$ electron with a total j of $\frac{3}{2}$.

a	$4s\,^24p(\frac{1}{2})-4s\,^24d(\frac{3}{2})$
b	$4s\,^24p(\frac{3}{2})-4s\,^24d(\frac{5}{2})$
c	$4s\,^24p(\frac{1}{2})-4s\,4p_-4p_+(\frac{1}{2})$
d	$4s\,^24p(\frac{3}{2})-4s\,4p_+4p_+(\frac{1}{2})$
e	$4s\,^24p(\frac{1}{2})-4s\,4p_-4p_+(\frac{3}{2})$
f	$4s\,^24p(\frac{3}{2})-4s\,^24d(\frac{3}{2})$

TABLE II. A comparison of the measured galliumlike transition wavelengths in the tokamak and the laser-produced plasma with wavelengths calculated by RELAC. Also, a comparison between the transition intensity as measured in the tokamak plasma and the prediction of a collisional-radiative model.

Transition	Tokamak wavelength (Å)	RELAC wavelength (Å)	Tokamak intensity	CR Model (10^{13} cm^{-3})	Laser-produced plasma wavelength (Å)
Pr XXIX					
a	87.7	87.76	100.0[a]	74	
b		105.65	[b]	24	105.23
c	125.7	123.29	20.0[c]	100	125.25
d		123.79	[c]	7	125.65
e	128.3	129.18	10.0[c]	75	128.44
Eu XXXIII					
a	77.9	77.00	100.0[a]	80	
b		105.65			
c	102.8	101.35	100.0	100	
d		123.79			
e	105.6	104.88	60.0	82	
Gd XXXIV					
a	74.1	73.26	100.0[a]	100	74.14
b		89.15		12	90.95
c	98.1	96.55	100.0	97	98.11
d		96.84		3	
e	100.6	99.66	60.0	81	100.45
Dy XXXVI					
a	67.5	66.74	a	100	
b		83.61		5	
c	89.1	87.71	83.0	72	
d		87.95		1	
e	90.9	90.13	100.0	62	
Yb XL					
a	57.4	56.08	a	100	
b		73.50		2	74.22
c	73.4	72.47	80.0	62	73.40
d		72.64		1	
e	74.5	73.96	100.0	57	74.56

[a]This transition is in the band produced by lower charge states; it is therefore difficult to measure its intensity.

[b]Blended with the copperlike $4s(J=\frac{1}{2})-4p(J=\frac{3}{2})$ transition.

[c]This transition is suppressed due to excitation-autoionization processes.

takamak spectrum lets one know whether low or high charge states are emitting along the line of sight in the plasma. On the other hand, time-integrated laser-produced plasma spectra obscure the spatial and time separation of various emitting charge states.

ATOMIC STRUCTURE CALCULATIONS AND COLLISIONAL RADIATIVE MODELS

Ab initio atomic structure calculations have been performed for copper-, zinc-, and galliumlike praseodymium, europium, gadolinium, dysprosium, and ytterbium using the parametric potential code RELAC, the relativistic version of MAPPAC [25]. Using the HULLAC package developed at Hebrew University and Lawrence Livermore Laboratory, a collisional-radiative model has been constructed for the copper-, zinc-, and galliumlike ion of each of the five atoms mentioned above [26].

Table I lists the transitions between the ten energy levels derived from the configurations $4s4p^2$ and $4s^24d$ and the levels of the ground-state doublet in the galliumlike ions calculated using RELAC.

To study the use of high charge states of transition metals as probes of transport phenomena in the plasma, the relative abundance of gallium-, zinc-, and copperlike ions must be estimated. From our collisional-radiative models for each charge state, we create synthetic spectra of the copper-, zinc-, and galliumlike ions emitted in coronal equilibrium using relative abundances for the various ions extracted from the literature [3,28]. The relative abundance of an ion X^Z to the next highest charge state X^{Z+1} is determined by the ratio of the total ionization rate from X^Z to X^{Z+1} to the total recombination rate from X^{Z+1} to X^Z. The terms in the ionization rate include direct collisional ionization and excitation autoionization, and the terms in the recombination rate include radiative and dielectronic recombination.

As is pointed out in Ref. [3], excitation-autoionization processes greatly suppress the galliumlike spectra of the lower-Z rare-earth atoms, namely, praseodymium, europium, and gadolinium. There are strongly autoionizing channels from the galliumlike charge states through $3d^94s^24p4f$ excited levels into zinclike $4s^2$ and $4s4p$ levels [3,27]. These excitation-autoionization channels grow progressively weaker as Z increases, until, at $Z = 66$, they become negligible as the autoionizing levels dip below the ionization limit.

For zinc- and galliumlike charge states of praseodymium and dysprosium, models of relative abundances have been created in Ref. [3], where an *ab initio* calculation by RELAC of autoionization rates was combined with standard approximations for direct ionization and radiative and dielectronic recombination. The model for dysprosium in that work is for a range of electron temperatures which we find too low for the present work. In this paper, the relative abundance of copper- to zinc- and zinc-to galliumlike ions is taken from Ref. [28]. The model of charge state distributions found in Ref. [28] uses semiempirical fits to relativistic distorted-wave approximation cross sections for electron-impact ionization, Kramer's classical cross section for radiative recombina-

tion, and the Burgess and Merts formula for dielectronic recombination rates, as well as a semiempirical, *ad hoc* augmentation of ionization rates to account for excitation-autoionization effects in elements with $Z \le 64$.

RESULTS AND DISCUSSION

Table II lists measured and calculated wavelengths and intensities for transitions *a*, *b*, *c*, *d*, and *e* for elements with Z's between 59 and 70. The data for praseodymium are calculated at T_e equal to 600 eV for europium at 800 eV, gadolinium at 1000 eV, dysprosium at 1.6 keV, and ytterbium at 2.0 keV. The temperatures used in the calculation of the spectra of the galliumlike ion of praseodymium, europium, and gadolinium are lower than usually assumed for maximum abundance, which reflects including excitation-autoionization processes in ionization balance calculations [28]. Because the excitation-autoionization channels are quenched for $Z \ge 66$, only collisional ionization and radiative and dielectronic recombination are included in the ionization balance calculation. Such a calculation predicts a maximum abundance of Dy^{35+} and Yb^{39+} at a temperature under 1 keV. These temperatures contradict what is seen in the experiments. Thus the calculations of the temperatures of maximum abundance used here for dysprosium and ytterbium were modified by an *ad hoc* enhancement of the dielectronic recombination rate, which served to raise the predicted temperatures [28] (explained in more detail below). All intensities are normalized to the brightest
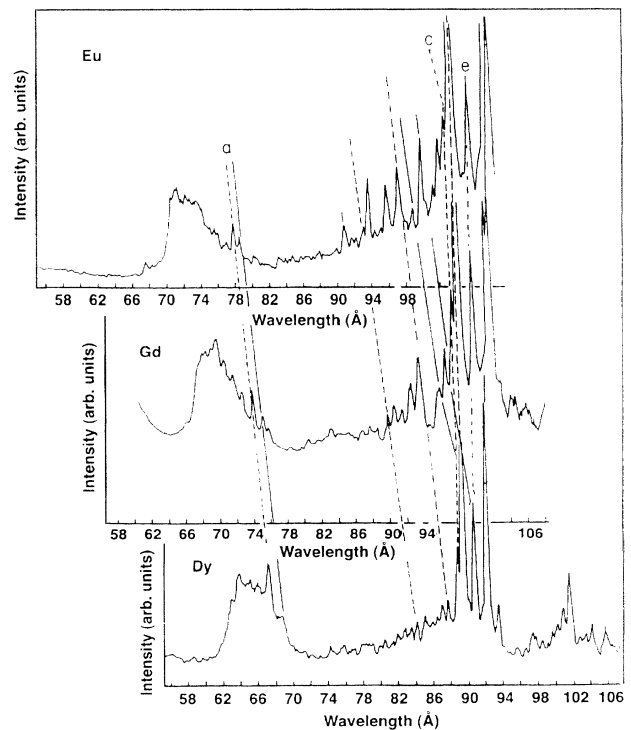

FIG. 4 Soft-x-ray emission pattern of three rare-earth elements, Eu, Gd, and Dy. The frame shown for each element is that of maximum emission in the galliumlike *e* line. Labeled transitions are identified in Table I.

line in the spectrum of each ion.

Figure 4 shows the isoelectronic trends of the stronger galliumlike lines of europium, gadolinium, and dysprosium in the tokamak spectra. The three strong transitions, $4s^2 4p(\frac{1}{2}) - 4s^2 4d(\frac{3}{2})$, $4s^2 4p(\frac{1}{2}) - 4s 4p_{1/2} 4p_{3/2}(\frac{1}{2})$, and $4s^2 4p(\frac{1}{2}) - 4s 4p_{1/2} 4p_{3/2}(\frac{3}{2})$, (a, c, and e as named in Table I, respectively) are identified in both tokamak and laser-produced plasma spectra. There is another $4p$-$4d$ transition, b, and several other $4s$-$4p$ transitions, such as d, predicted to lie near these three in wavelength (discussed below), but only a, c, and e were predicted to be bright in the tokamak spectra. This is not surprising as a, c, and e are fed collisionally from the ground state, where there is always a large population. However, as the density of the plasma increases the upper state in the $4s^2 4p$ doublet, $^2P_{3/2}$, is collisionally populated faster than its $M1$ decay to the ground state can depopulate it. As a result, b and d are predicted to become increasingly bright compared to a, c, and e. Thus emission from lines b and d can serve as density diagnostics between 10^{12} and 10^{16} cm^{-3}. Emission features b and d are seen in the laser-produced plasma, but due to the large uncertainty in the brightness measurements on the photographic plates they are only entered in Table II as wavelengths, and no statement is made regarding their intensities.

Figure 5 shows the predicted behavior of the brightness of transitions c and e (top) and b and d (bottom) relative to transition a (which remains strong at all densities, and for all elements, analyzed here) as a function of electron density. (Since opacity affects the brightness of resonance lines at densities above 10^{19} cm^{-3}, calculations above 10^{16} cm^{-3} included escape factors for a plasma 250 μm thick and with the ion temperature nearly equal to the electron temperature.) The transitions c and e are close in wavelength to each other and are well separated from transition a. The figure serves to illustrate the behavior of the galliumlike lines for these ions in a crowded spectral region as a function of free-electron density. This behavior of these ratios is very similar for all of the ions considered here, even praseodymium, the only difference being that in the models, a is not consistently the strongest emission feature as a function of density for $Z < 64$. The figure also shows the experimental (tokamak) value of the c/a and e/a ratios along with a 60% uncertainty in the measured brightness reflecting the uncertainty in the estimate of the a line intensity. This line always "sits" on the quasicontinuum generated by the lower charge states with $4p^6 4d^k$ ground configurations. Since the laser spectra are not photometrically calibrated and the intensity estimates are limited
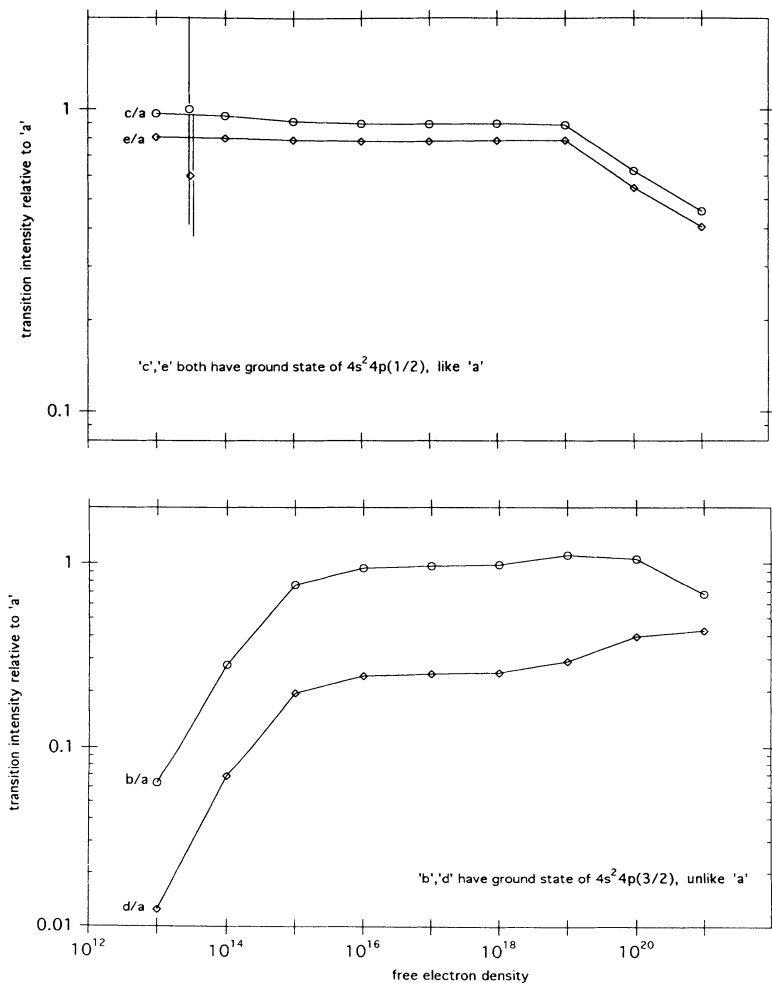

FIG. 5. The calculated electron-density dependence of galliumlike transition emissivities between 10^{13} and 10^{21} cm^{-3}. The top frame is of the ratio of Gd XXXIV c and e to a at $T_e = 800$ eV and the bottom frame is b and d to a also at $T_e = 800$ eV. Labeled transitions are identified in Table I. Opacity effects strongly determine the shape of the ratios for b and d above 10^{19} cm^{-3}.

by the crude model used to account for opacity, we did not compare the experiment with the prediction in Fig. 5.

As was reported in Ref. [3], excitation-autoionization processes make observations of the brightness of gallium-like praseodymium and europium emission features very difficult because the fractional abundance of the charge state is greatly suppressed. While it is very difficult to measure accurately the intensity of a for praseodymium in the presence of emission from lower charge states, it is straightforward to compare the intensities of lines c and e for praseodymium. The agreement between the measured relative brightness of praseodymium emission features c and e in the tokamak spectra and the predicted relative brightness of the features in the collisional-radiative (CR) model is quite good. Good agreement is achieved between the measured line intensities in the tokamak and the predictions of the collisional-radiative model for europium and gadolinium.

From praseodymium to gadolinium, the brightness of transition c is always greater than that of e in the tokamak spectra. This brightness is observed to reverse in relative strength for dysprosium and ytterbium (see

Table II). The collisional-radiative model calculation predicts that for all Z, the value of the brightness of c will be greater than the value of the brightness of e, but the discrepancy between theory and experiment is small compared to the 30% uncertainty in the brightness measurements of each line.

RELAC calculations reveal that as Z increases from praseodymium to europium, the $4s^2 4d_{3/2,5/2}$ levels decrease in energy relative to the $4s(4p_{3/2})^2$ $J = \frac{1}{2}, \frac{3}{2}$, and $\frac{5}{2}$ levels. Figure 6 shows the energy-level diagrams for some of the first 12 levels of Pr^{28+}, Gd^{33+}, and Yb^{39+}, respectively. (The corresponding diagrams for Eu^{32+} and Dy^{35+} would look just like that of the gadolinium ion.) Note the crossing between the $4s^2 4d_{3/2}$ level and the $4s(4p_{3/2})^2$ complex that occurs between Pr^{28+} and Gd^{33+} and between the $4s^2 4d_{5/2}$ level and the $4s(4p_{3/2})^2$ complex that occurs between Gd^{33+} and Yb^{39+}. The level crossings shown here between the $4s^2 4d$ complex and the $4s(4p_{3/2})^2$ complex cause predicted shifts in position relative to each other of the galliumlike transitions b, f, and d, identified in Table I. That is, in Table II, b is shorter
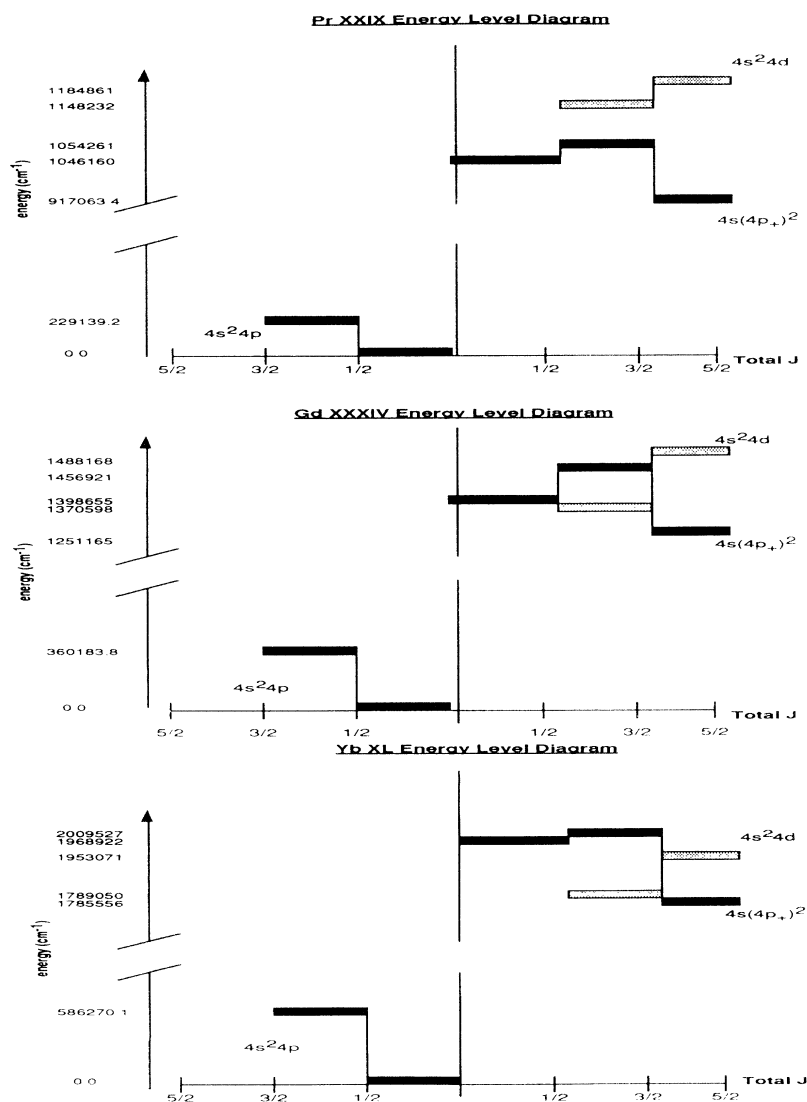

FIG. 6. Energy-level diagram for some of the first 12 levels of Pr^{28+}, Gd^{33+}, and Yb^{39+}. Levels shown come from the $4s^2 4p$, $4s(4p_{3/2})^2$, and $4s^2 4d$ configurations. Odd-parity levels are on the left-hand side of the center line, even-parity levels are on the right.
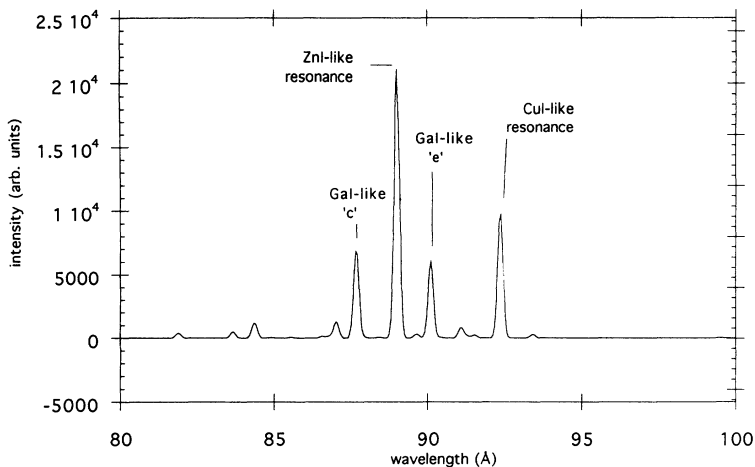
FIG. 7. Synthetic spectrum for the rare-earth element dysprosium showing emission from gallium-, zinc-, and copperlike charge states. The spectrum is calculated at $T_e = 1.6$ keV for all charge states and with $n_e = 3.0 \times 10^{13}$ cm^{-3}. All charge states in this spectrum have been given equal relative abundance.

in wavelength than d for Pr^{28+} but longer in wavelength than d for Yb^{39+}. All three of these transitions end on the $4s^2 4p_{3/2}$ level; thus the energy ordering of their upper states determines the ordering of their wavelengths. The observed shift of the wavelength of transition b with respect to that of transition c (b is much shorter than c for praseodymium, and longer than c for ytterbium) on the other hand is due to the increased splitting of the two $4s^2 4p$ ground levels. A similar effect should have been seen for transitions f and e. Unfortunately, f was too faint to allow for a wavelength measurement to be reported here.

Figure 7 is a synthetic spectrum of dysprosium with copper-, zinc, and galliumlike ions present and with adjacent charge states coupled through ionization balance calculations as described above. The spectrum is calculated with an electron temperature of 1600 eV for the gallium-, zinc-, and copperlike charge states, and with an electron density of 3.0×10^{13} cm^{-3}. Emission features of gallium-, zinc-, and copperlike dysprosium are barely measurable in plasmas with core temperatures of 1.0 to 1.2 keV, as shown in Fig. 8. As one can see by comparing Figs. 7 and 8, given the conditions used in the synthetic spectrum, the model agrees well with the experimental spectrum. The discussion of the relative abun-

dance of the three charge states has been briefly presented in Ref. [28]. As is mentioned above, this implies that our initial estimate of a temperature of maximum fractional abundance for galliumlike dysprosium of under 1 keV is too low. The calculation for the relative brightness of emission features in Table II was done at a "modified" electron temperature of 1.6 keV; the intensities in Table II are relative intensities and are insensitive to changes of a factor of a few in temperature. This work is currently being developed in another paper.

CONCLUSION

Soft-x-ray spectra of highly ionized rare-earth atoms have been recorded from tokamak and laser-produced plasmas. The transitions between ground, $4s^2 4p$, and excited $4s 4p^2$ and $4s^2 4d$ states in galliumlike ions have been studied by comparison of the experimental data with predictions of $ab\ initio$ energy-level calculations and collisional-radiative models. Three transitions, a, c, and e, fed by the $4s^2 4p(\frac{1}{2})$ true ground state have been identified in both plasmas. Predictions of the brightness ratios of these emission features at low densities and low Z agree well with experimentally measured ratios. At higher densities, opacity effects and blending make the
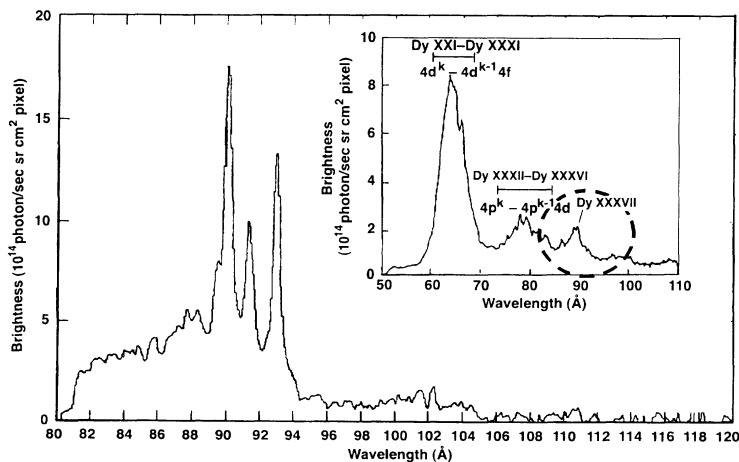

FIG. 8. Two experimental spectra of dysprosium. Upper frame: recorded from a plasma with a core temperature of 1.0 keV. Note the weakness of the gallium-, zinc-, and copperlike emission features in the 85–95-Å range. Bottom frame: recorded in a plasma with a core temperature of 1.5 keV. This spectrum is a blow up of the 85–95-Å range where the gallium-, zinc-, and copperlike emission features are found. Both spectra are on the same absolute brightness scale.

comparison difficult.

We also identify in the laser plasma two transitions, *b* and *d*, fed from the higher energy $J = \frac{3}{2}$ component of the ground configuration. These transitions exhibit a strong density dependence in their emission brightness. A sixth transition, $4s^24p(\frac{3}{2})-4s^24d(\frac{3}{2})$, was too faint to be measured.

For each rare-earth ion, calculations of the energy-level structure and scaling as a function of Z need a fully relativistic atomic structure code. Our studies reveal level crossing in galliumlike ions that cause a corresponding reordering of their emission features. Also, isoelectronic trends in the ground term doublet splitting of these ions were studied. Agreement between our results at high Z's and previously published results at lower Z's was found for the ground-state fine structure of these ions.

Another point of this study is to lay the ground work to see if galliumlike emission features can be used in comparison to zinc-, and copperlike emission features as a diagnostic measure of transport phenomena in tokamak plasmas. By using a detailed ionization equilibrium model, we were able to construct an accurate model of the charge state distribution in the plasma under equilibrium conditions. Comparisons made between models for dysprosium and the experiment are in agreement, and will be discussed in more detail in a forthcoming paper.

[1] S. Maxon, P. Hagelstein, J. Scofield, and Y. Lee, J. Appl. Phys. **59**, 293 (1986).
[2] B. J. MacGowan, S. Maxon, P. Hagelstein, C. J. Keane, R. A. London, D. L. Matthews, M. D. Rosen, J. H. Scofield, and D. A. Whelan, Phys. Rev. Lett. **59**, 2157 (1987).
[3] P. Mandelbaum, M. Finkenthal, E. Meroz, J. Schwob, J. Oreg, W. Goldstein, M. Klapisch, L. Osterheld, A. Bar-Shalom, S. Lippmann, L. K. Huang, and H. W. Moos, Phys. Rev. A **42**, 4412 (1990).
[4] P. K. Carrol and G. O'Sullivan, Phys. Rev. A **25**, 275 (1982).
[5] M. Finkenthal, H. W. Moos, A. Bar-Shalom, N. Spector, A. Zigler, and E. Yarkoni, Phys. Rev. A **38**, 288 (1988).
[6] M. Finkenthal, S. Lippmann, L. K. Huang, H. W. Moos, Y. Lee, N. Spector, A. Zigler, and E. Yarkoni, Phys. Scr. **41**, 445 (1990).
[7] P. Mandelbaum, M. Finkenthal, J. L. Schwob, and M. Klapisch, Phys. Rev. A **35**, 5051 (1987).
[8] M. Finkenthal, S. Lippmann, L. K. Huang, T. L. Yu, B. Stratton, H. W. Moos, M. Klapisch, P. Mandelbaum, A. Bar-Shalom, W. Hodge, P. Phillips, T. R. Price, J. Porter, B. Richards, and W. Rowan, J. Appl. Phys. **59**, 3644 (1986).
[9] W. Hodge, M. Finkenthal, H. W. Moos, S. Lippmann, L. K. Huang, A. Bar-Shalom, and M. Klapisch, J. Phys. (Paris) Colloq. **49**, C1-75 (1988).
[10] J. Reader and G. Luther, Phys. Scr. **24**, 732 (1981).
[11] G. Doschek, U. Feldman, C. Brown, J. Seely, J. Ekberg, W. Behring, and M. Richardson, J. Opt. Soc. Am. B **5**, 243 (1988).
[12] E. Hinnov, P. Beiersdorfer, R. Bell, J. Stevens, S. Suckewer, S. von Goeler, A. Wouters, D. Dietrich, M. Gerassimenko, and E. Silver, Phys. Rev. A **35**, 4876 (1987).
[13] J. Reader and G. Luther, Phys. Rev. Lett. **45**, 609 (1980).
[14] N. Acquista and J. Reader, J. Opt. Soc. Am. B **1**, 649 (1984).
[15] J. Reader, N. Acquista, and S. Goldsmith, J. Opt. Soc. Am. B **3**, 874 (1986).
[16] U. Litzén and X. Zeng, Phys. Scr. **43**, 262 (1990).
[17] A. Trigueiros, C. J. B. Pagan, and J. G. Renya Almandos, Phys. Rev. A **38**, 166 (1988).
[18] L. Curtis, J. Reader, S. Goldsmith, B. Denne, and E. Hinnov, Phys. Rev. A **29**, 2248 (1984).
[19] L. Curtis and P. Ramanujam, Phys. Scr. **27**, 417 (1983).
[20] L. Curtis, Phys. Rev. A **35**, 2089 (1987).
[21] S. A. Cohen, J. Cecchi, and E. Marmar, Phys. Rev. Lett. **35**, 1507 (1975).
[22] K. Gentle, R. Bengtson, R. Bravenec, D. Brower, W. Hodge, T. Kochanski, N. Luhmann, Jr., D. Patterson, W. Peebles, P. Phillips, E. Powers, T. Price, B. Richards, C. Ritz, D. Ross, W. Rowan, R. Savage, J. Wiley, and Y. Wan, Plasma Phys. Control. Fusion **26**, 1407 (1984).
[23] W. Hodge, B. Stratton, H. W. Moos, Rev. Sci. Instrum. **55**, 16 (1984).
[24] A. Filler, J. Schwob, and B. Fraenkel, in *Proceedings of the Fifth International Conference on Vacuum Ultraviolet Radiation Physics, Montpellier, 1977*, edited by M. Castex, M. Pouey, and N. Pouey (CNRS, Paris, 1977), p. 86.
[25] M. Klapisch, Comput. Phys. Commun. **2**, 269 (1971); M. Klapisch, J. L. Schwob, B. S. Fraenkel, and J. Oreg, J. Opt. Soc. Am. **67**, 148 (1977).
[26] K. Fournier, W. Goldstein, A. Osterheld, M. Finkenthal, C. Holmes, and H. W. Moos, UCRL Report No. 115497 (1993) (unpublished).
[27] J. Oreg, W. Goldstein, P. Mandelbaum, D. Mitnik, E. Meroz, J. Schwob, and A. Bar-Shalom, Phys. Rev. A **44**, 1741 (1991).
[28] M. Finkenthal, A. Zwicker, L. K. Huang, S. Lippmann, H. W. Moos, Y. Lee, W. H. Goldstein, A. Osterheld (unpublished).
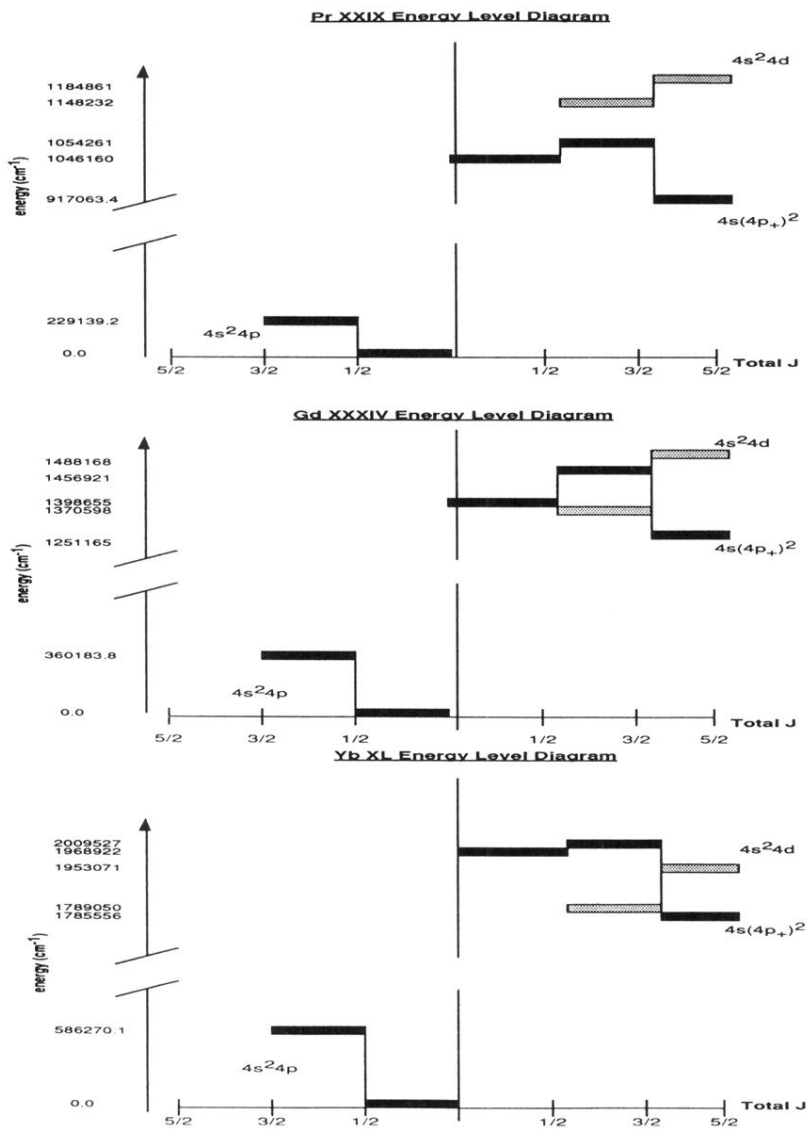
Pr XXIX Energy Level Diagram

Gd XXXIV Energy Level Diagram

Yb XL Energy Level Diagram

FIG. 6. Energy-level diagram for some of the first 12 levels of Pr^{28+}, Gd^{33+}, and Yb^{39+}. Levels shown come from the $4s^2 4p$, $4s(4p_{3/2})^2$, and $4s^2 4d$ configurations. Odd-parity levels are on the left-hand side of the center line, even-parity levels are on the right.